THREE–DIMENSIONAL ANALYSIS OF THE PORE STRUCTURE OF CEMENT–BASED MATERIALS

Wenjie Zhou **Supervisor: Dr. H.S. Wong**

Concrete Durability Research Group, Department of Civil and Environmental Engineering, Imperial College London.

1. Introduction

The characteristics of the pore structure play a major role in controlling the transport properties and durability of cement-based materials. The aim of this project is to quantify these characteristics in 3D by means of image analysis.

Objectives:
- Acquire 3D images of pore structures in cement paste by applying a serial section and imaging method with laser scanning confocal microscopy (LSCM).
- Develop applicable threshold algorithms to extract the pore structure - from reconstructed images for 3D quantification of the characteristics.
- Work out an appropriate way to quantify the characteristics of the pore structure.
- Understand the correlation between the parameters.

2. LSCM

3D imaging of the cement-based materials are required for the identification of the pore structure. For this project LSCM is applied for imaging the samples, the adoption of LSCM (shown in Figure 1) enables elimination of out-of-focus light, increases resolution, improves contrast, allows for multi-channel imaging of co-localised objects, and enables non-invasive section scanning and imaging of thick specimens (He *et al*., 2006).

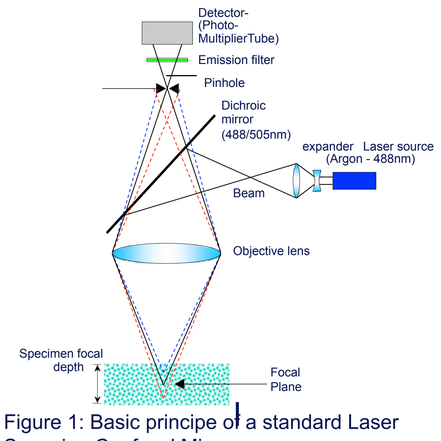

Figure 1: Basic principe of a standard Laser Scanning Confocal Microscopy. *(Source: Confocal imaging of porosity in hardened concrete)*

3. Sample preparation and LSCM settings

The two cement paste samples we used for this project are CEM I and CEM I + 60% GGBS cement pastes. Method described in Wong and Buenfeld (2006) was applied to remove the pore water by de-airing and impregnating the block with fluorescent epoxy resin for imaging. The composition of the two samples is given in Table 1 below.

Table 1. Cement paste samples composition and age

	CEM I (%)	GGBS (%)	w/c ratio	Age (days)
CEM I	100	0	0.45	7
GGBS	40	60	0.45	7

An argon laser with a wavelength of 488 nm was applied to excite fluorophores. A beam splitter ranging from 500 to 600 nm was used to collect the emitted fluorescence at the photomultiplier tube (PMT). A 40× (NA 1.25) oil immersion objective and a field of view of 387 × 387 μm^2 was used in all cases. In order to obtain images with high resolution, specific imaging settings were applied shown in Table 2 below.

Table 2. Imaging settings of LSCM

Pinhole (Airy unit)	Spatial *XY* resolution (μm)	Spatial *Z* resolution (μm)	Scan format	Zoom	Voxel size (X × Y × Z) (μm3)
0.3	0.156	0.534	2048 × 2048	1.8×	0.105 × 0.105 × 0.1

4. Serial sectioning and 3D image reconstruction

This method (shown in Figure 2) was developed by Yio *et al*. (2015) for imaging 3D volumes of cement-based material ensuring that sequential serial sections in the z-stack would share an overlapping area for the stitch.

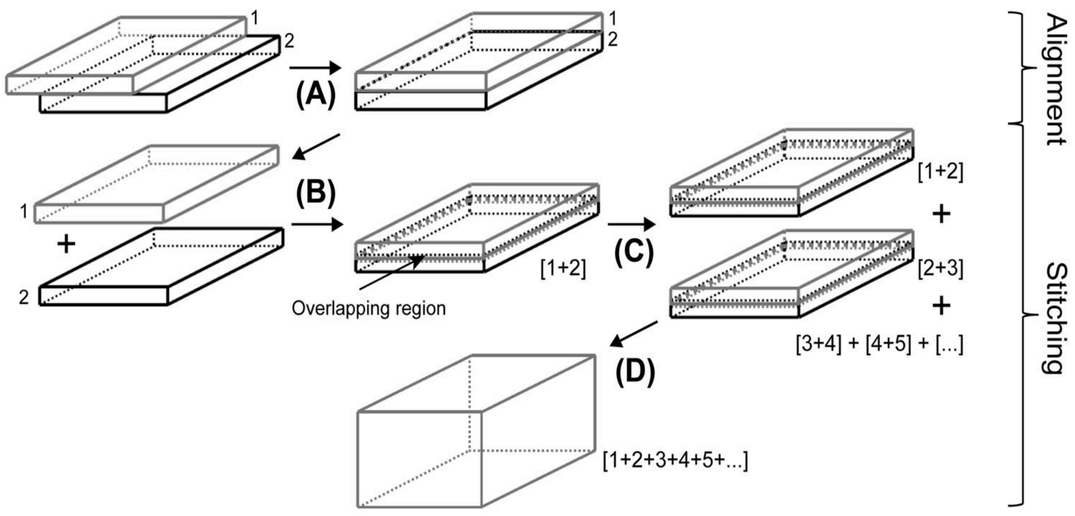

Figure 2: Stitching process. (A) Selected images from each z-stack are aligned; (B) Stitched in pairs; (C) Combined z-stacks (i.e. [1+2] + [2+3] + [3+4] + [4+5] + […]) by stitching the overlapping regions progressively (D) Reconstruct an image volume. *(Source: 3D imaging of cement-based materials at submicron resolution by combining laser scanning confocal microscopy with serial sectioning)*

5. Pore structure extraction

Two thresholding algorithms that are based on the 'overflow' method (Wong, 2006) are developed, both were aimed at finding the inflection point of the cumulative curve (shown in Figure 3).

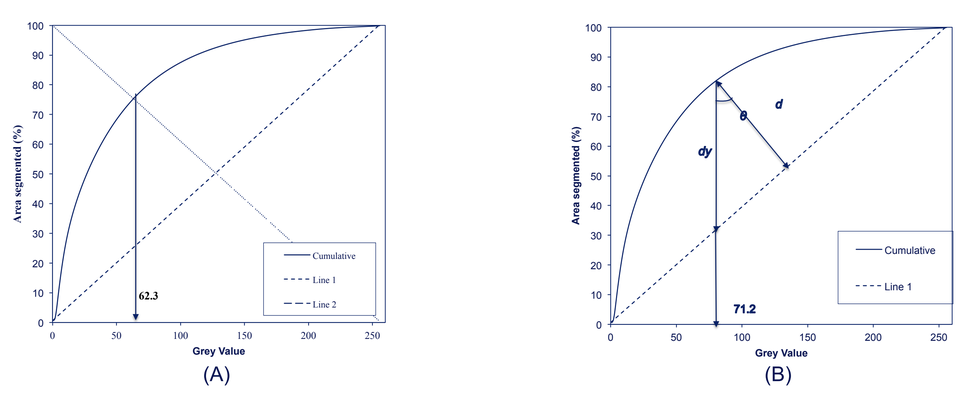

Figure 3: Plot of cumulative grey scale histogram for GGBS – A1 and thresholding algorithms: (A) Method 1 : Draw diving line and (B) Method 2 : Find the maximum perpendicular distance between the curve and straight line.

6. Validation of skeletonisation algorithm

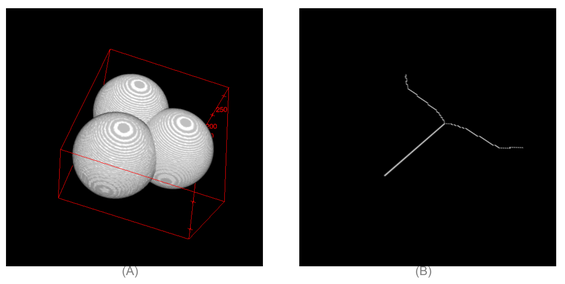

Figure 4: (A) 3D model of three spheres join together, and (B) skeleton of the model

Validation of skeleyonisation algorithm is achieved by simulating 3D composite of three pores join together in the pore structure of a cement-based material (Figure 4A). The successfully outlined the composite with three lines, which acted as three medial axis of the drainage pathway, joined at a single point (Figure 4B).

7. Pore structure reconstruction

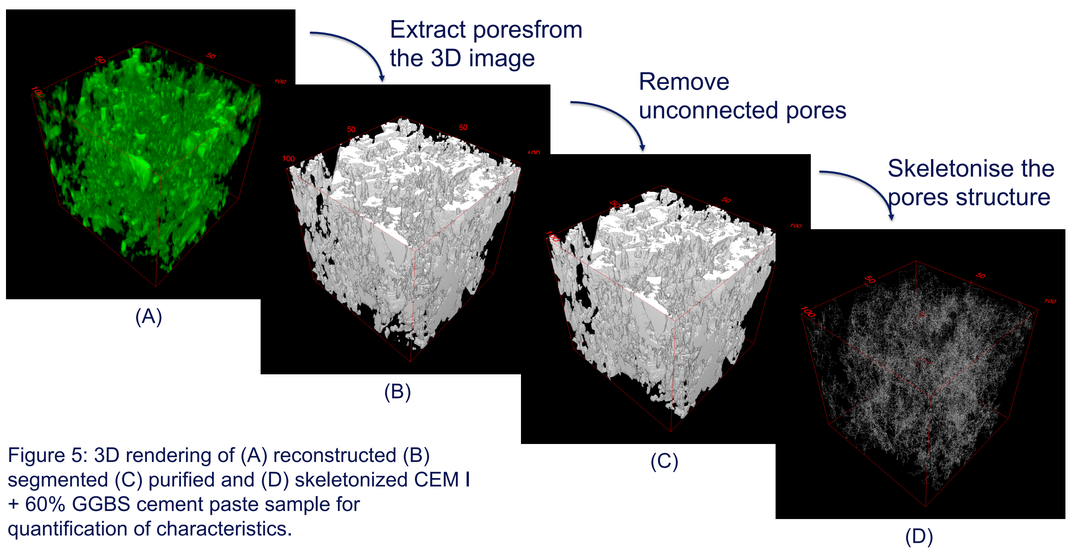

Figure 5: 3D rendering of (A) reconstructed (B) segmented (C) purified and (D) skeletonized CEM I + 60% GGBS cement paste sample for quantification of characteristics.

8. Quantification of the pore structure

Results of the quantification of the pore structure are shown in Table 3, these results were used to analyse the possible factor that will affect the results such as different sampling size and imaging location.

Table 3: Pore characteristics of cement paste samples as determined from LSCM (M1: Method 1; M2: Method 2).

Sample	Porosity (-)		Tortuosity (-)		Connectivity ($\times 10^{16}$) (m^{-3})		Surface Area ($\times 10^{10}$) (m^2*m^{-3})		Nodes density ($\times 10^{16}$) (m^{-3})		Length density ($\times 10^{10}$) ($m*m^{-3}$)		Branches density ($\times 10^{16}$) (m^{-3})	
	M1	M2	M1	M2	M1	M2	M1	M2	M1	M2	M1	M2	M1	M2
CEM I-A1	26.62	18.74	1.32	1.31	3.85	2.69	28.44	22.51	8.93	11.85	25.81	16.92	16.43	11.85
CEM I-A2	26.62	19.86	1.32	1.31	3.89	2.91	28.53	23.76	9.02	12.83	24.52	18.34	16.6	12.83
CEM I-B1	28.82	18.78	1.34	1.34	4.57	3.15	26.24	21.14	9.85	13.13	26.02	18.13	18.21	13.13
CEM I-B2	26.68	20.34	1.34	1.33	4.63	3.76	27.29	24.02	10.24	15.58	27.12	21.59	18.84	15.58
Mean	27.19	19.43	1.33	1.32	4.24	3.13	27.62	22.86	9.51	13.35	25.87	18.75	17.52	13.35
GGBS-A1	25.27	21.36	1.35	1.35	3.44	2.81	22.37	19.38	7.52	11.66	20.79	17.04	13.94	11.66
GGBS-A2	26.48	23.05	1.37	1.34	3.33	2.73	24.31	21.6	7.63	11.99	21.31	18.03	14.19	11.99
GGBS-B1	24.79	22.71	1.35	1.35	3.93	3.52	22.03	20.74	8.28	14.08	22.3	20.1	15.48	14.08
GGBS-B2	27.23	23.81	1.34	1.34	3.69	3.25	24.72	22.47	8.25	13.58	22.82	19.93	15.25	13.58
Mean	25.94	22.73	1.35	1.34	3.59	3.08	23.36	21.05	7.92	12.83	21.8	18.77	14.72	12.83

9. Conclusion

- Accuracy of the segmentation algorithms could not be determined due to lack of reference values.
- Sampling size had a small effect on porosity compare to tortuosity.
- A positive correlation was found between tortuosity and surface area.
- No correlation was found between tortuosity and porosity and also between tortuosity and connectivity.
- Spatial variability could not be determined due to lack of data connected.

10. Reference

He, L., Zhang, S., Xiao, C. Y. & Chen, Y. Z. (2006) *Segmentation of LSCM Images based on Multi- channel Information Fusion.*
Raheem, S., Nahil, S., Umberto, R., Gabriel, P. & Mohamed, M. (2015) *ImageJ.*
Wong, H. S. (2006) Pore segmentation of cement-based materials from backscattered electron images. *Cement and Concrete Research.* 36 (6).
Wong, H.S. & Buenfeld, N.R. (2006) Patch microstructure in cement-based materials: fact or artefact? *Cement Concrete Res*. 36, 990–997.
Yio, M. H. N., Mac, M. J., Wong, H. S. & Bunfeld, N. R. (2015) 3D imaging of cement-based materials at submicron resolution by combining laser scanning confocal microscopy with serial sectioning. *Journal of Microscopy.*